SCANS Computer Program for Evaluating Lead Slump and Buckling in Storage and Transportation Casks*

G.C. Mok, T.Y. Lo, M.C. Witte, R.C. Chun

Lawrence Livermore National Laboratory, Livermore, California, United States of America

INTRODUCTION

SCANS is a computer program developed for the U.S. Nuclear Regulatory Commission and the U.S. Department of Energy for making confirmatory stress analyses of transportation casks submitted for license review. The program, running on IBM PC and compatible microcomputers, handles heat transfer, impact, thermal and pressure stress analyses. To minimize the need for the user's familiarity with current licensing regulations and computerized analysis techniques, the computer program automatically generates and archives the required input and output files based on a minimum amount of engineering data enter interactively by the user. This automated option is for a generic circular cylindrical cask geometry to meet the U.S. 10 CFR 71 regulations. The first version of this program has been released to the public since January 1989. A workshop and a number of papers have been given by the developer, Lawrence Livermore National Laboratory concerning the methods and applications of this program.

This paper describes the results of a new development in the impact analysis capability of this program not previously reported. Specifically, the paper examines the effect of lead slump on the buckling strength of a circular cylindrical cask with lead shield. It shows that slumping of the lead shield seriously degrades buckling strength. To facilitate the presentation of this result, the paper first describes the lead slump and buckling phenomena, then highlights SCANS simplified methods for the analysis of these phenomena. To confirm the validity of these methods, the paper compares SCANS results to those of tests and other computer programs. Finally, the validated methods are applied to demonstrate the possible effect of lead slump on the buckling strength of a typical rail transportation cask.

LEAD SLUMP AND SCANS ANALYSIS METHOD

Figure 1 depicts a meridional cross section of a typical circular cylindrical cask undergoing an end-on impact. The cylindrical body of the cask is made of three concentric shells; the lead shield located in the middle is protected by the outer and inner steel shells. As shown in the left half of Fig. 1, if the lead and steel shells can be bonded perfectly, the three shells will act as an integral structure and the strength of the steel will provide axial support to the lead shield during the end-on drop. Otherwise, as demonstrated in the right half of Fig. 1, the lead receiving support only in the lateral direction may deform excessively and plastically under the axial impact load, resulting in the phenomenon commonly called lead slump. This phenomenon has two major consequences. First, a permanent gap may appear in the lead shield at the end of the package opposite the impact and allow radiation to leak outside. Second, the slumping lead would exert a lateral pressure on the inner and

* This work was supported by the United States Nuclear Regulatory Commission under a Memorandum of Understanding with the United States Department of Energy.

outer steel shells and degrade the yield and buckling strengths of the steel shells. The second effect is the topic of this paper.

In practice, the condition of the bond between the lead and steel shells is difficult to assess. Hence the effect of possible lead slump under impact load must be investigated to assure the safety performance of the cask. For this investigation, SCANS uses a simplified methodology conservatively assuming that the lead and steel are totally unbonded. The method of lead slump analysis has been detailed in Chun et al. 1989 and Mok et al. 1989, but for the convenience of the reader of this paper, a synopsis of the method is given here. Figure 2 presents the SCANS analytical model for the lead slump analysis. The model comprises three submodels: one beam model for the lateral motion and two spring models for the axial motion. Since the steel shells completely surround the lead shield in the lateral directions, it is reasonable to assume that the entire cask body, whether bonded or unbonded, moves together in these directions as a composite structure. Thus, one composite beam model suffices for the analysis of the lateral motion. However, for the axial motion, two models are required, one for the lead shield and the other for the steel shells. Since the two steel shells are joined at the two ends, their axial motions are approximately the same and can be described by the one model. The impact ends of all three submodels are connected to the impact point by a rigid link depicted by a dashed line in Fig. 2. The two axial models are coupled in the radial direction of the cask, and the coupling relation satisfies the equilibrium conditions of the radial forces and the continuity or compatibility conditions of radial displacements at the lead-steel interfaces. As shown in Mok et al. 1989, these conditions and the stress-strain relations of the lead and steel shells provide 20 equations for 22 unknowns. By treating the two axial strains as known quantities, the 20 equations can be condensed to two equations relating the two axial strains to the two axial forces of the two axial models. Using these force-strain relations, the equation of motion of the two axial models are solved numerically to provide the results of axial forces and strains, which are then substitute into the 20 equations to find the detailed stresses in the lead and steel shells. The two axial spring models produce all the results affected by the lead slump, and the beam model merely describes the global impact motion of the cask. The lead slump affects only the local distribution of forces and deformations but not the global motion of the cask. When the lead and steel shells are perfectly bonded, lead slump does not occur and all shells move together as a composite beam in all directions. For this case, only one beam model suffices for the analysis of the impact motion and stress of the cask. Figure 3 shows this model used in SCANS.

Despite the simplicity of the model for lead slump analysis, the SCANS computer program produces fairly accurate predictions of the stresses caused by lead slump. This conclusion can be seen in the results presented in Table 1, which compares SCANS results to those of the NIKE computer program. The results are for a typical rail cask whose geometry and force-deflection curve of the impact limiters are given in Figures 4 and 5. NIKE is a general-purpose finite-element program capable of obtaining accurate detailed results for stress due to impact. The 2-D finite-element model used to obtain the NIKE results in Table 1 is shown in Fig. 6. The model, made of axisymmetric solid elements, uses two elements over the radial thickness and 50 elements over the axial length of each shell. The NIKE results presented in Table 1 are the average stresses over the shell thickness. Table 1 shows that the NIKE and SCANS results compare closely for both bonded and unbonded lead shields and for a wide variation of the Young's modulus of lead. Table 1 also shows that the lead slump produces a high hydrostatic pressure in the lead, a high compressive hoop stress in the inner steel, and a high tensile hoop stress in the outer steel shell. A study reported in Mok et al. 1989 using the NIKE model further shows that the magnitude of the lead-slump stresses in the steel shells is determined mainly by the effective modulus of the lead and is insensitive to the extent of plastic deformation in the lead. Thus, the SCANS elastic model can still be used to predict lead-slump stresses even after the lead shield yields.

When combined with the axial compressive impact stress, the compressive hoop stress produced by lead slump in the inner steel shell of a cask can drastically lower the buckling strength of the shell. To assess this effect, the recently implemented buckling analysis capability of SCANS is used. The following section gives a brief description of the basis and verification of this analysis capability of the program.

BUCKLING AND SCANS ANALYSIS METHOD

Buckling is a structural failure produced by compressive stress. A structure is buckled when it becomes unstable under the stress. The instability can be a rapid increase of the deformation or a sudden loss of the load-carrying capacity of the structure. Such structural instability can seriously damage the containment and subcriticality of casks containing radioactive materials. The buckling stress limit of a structure depends not only on the structure's material properties but also on the geometry. A cylindrical shell buckles quite differently from a bar or a plate. Similarly, a slender structure would buckle at lower stress than a thicker one. Figure 7 illustrates the various buckling behaviors of a circular cylindrical shell. This figure shows that the initial geometrical imperfections and the symmetry of the deformation have great effect on the buckling stress and behavior of the shell. A perfect shell with symmetrical deformation tends to buckle at relatively higher stress.

For structures of simple geometry such as bars, plates, and circular cylindrical shells, formulas for the calculation of elastic buckling stress have been obtained with the implicit idealized assumptions that the geometry is perfect, the material property is uniform, and the boundary condition is well defined, etc. These theoretical formulas can be found in textbooks and handbooks. However, in reality, the ideal conditions seldom exist, and the actual buckling stress can be quite different from the prediction of the theoretical formula if the buckling stress is sensitive to slight deviations from the ideal conditions, as has been demonstrated in Fig. 7 for the axial buckling stress of a circular cylindrical shell.

Because of the deficiency of the theoretical formulas for elastic buckling stress, correction factors are used with these formulas in design practice. Two correction factors are commonly used, namely, the capacity reduction factor α, and the plasticity reduction factor η The actual buckling stress limit σ_ℓ is given as a product of these two reduction factors and the theoretical elastic buckling stress, σ_e, i.e.,

$$\sigma_\ell = \alpha \eta \sigma_e. \qquad (1)$$

Both reduction factors in Eq. (1) have values between 0 and 1. Thus the actual stress limit never exceeds the theoretical elastic buckling stress. For circular cylindrical shells, the capacity reduction factor mainly represents the effect of initial geometric imperfections and the plasticity factor is for the effect of plastic deformations, which would appear when the buckling stress exceeds the elastic or proportional limit of the shell material.

For the buckling analysis of a circular cylindrical cask, the SCANS computer program follows the ASME Boiler and Pressure Vessel Code, Code Case N284. The analysis is first carried out for each of the stress components, namely, the axial, hoop, and shear stresses in the shell. For each stress, the theoretical elastic buckling stress is obtained using a textbook formula, then appropriate values of the capacity and plasticity reduction factors corresponding to the actual buckling stress are determined and inserted into Eq. (1) to find the actual buckling stress. A simple technique has been developed in Lo et al. 1989 to find the appropriate value for the plasticity reduction factor without iterations. To determine the adequacy of the shell to resist buckling under a given set of applied stresses, the applied stresses are compared first individually to the corresponding actual buckling stress. If none of the ratios of applied stress to actual buckling stress exceeds the value of 1.0; i.e., if the shell does not buckle under the individual stresses, then the possibility of buckling under combined stresses is checked, by inserting the ratios of applied stress to buckling stress into a set of interaction formulas. The detailed formulas and procedure for this analysis in SCANS are given in Lo et al. 1989.

Lo et al. 1989 also compares the formulas used by SCANS and by other major design codes and recommendations. It shows that the greatest differences among the various design codes occur in the results for the axial stress, not for the hoop and shear stresses. To show these differences, the present paper presents in detail the axial stress results and shows that the ASME-N284 method used in the SCANS computer program is consistent with and more conservative than other design codes.

Using Eq. (1) to find the actual buckling stress for a circular cylindrical shell under axial compression, the theoretical elastic buckling stress must first be obtained. For this purpose, all design codes use essentially the same formula, i.e.,

$$\sigma_e = CEt/R, \qquad (2)$$

where E is the Young's modulus of the shell material; t and R are the thickness and radius of the shell, respectively; and C is a coefficient that varies with the length parameter, $M = L/(Rt)^{1/2}$ of the shell. For the inner and outer steel shells of most shipping casks, M is greater than 1.73 and C is equal to $1/[3(1-\nu^2)]^{1/2}$. C is equal to 0.605, when the Poisson's ratio ν has a value of 0.3.

The capacity reduction factor, α used in Eq. (1) for axial buckling of a circular cylindrical shell is determined by test. Test results have shown that the capacity reduction factor decreases with increasing initial geometric imperfections of the shell. The imperfections can be introduced by the manufacturing process or by other causes. As an indication of the high sensitivity to imperfections, the test data show much scatter, which causes considerable differences in the values recommended by the various design codes for the capacity reduction factor. Figure 8 shows the scatter of the test data and the differences in the recommended values for the capacity reduction factor. The details of the test data can be found in Brush and Almroth 1975. The formulas to generate the curves for the American design codes (ASME N284, API-2U, ALCOA, and NASA) are given in Lo et al. 1989, and the formulas for the German code (DAST-Ri013) and the European code (ECCS-RP4.6) are described in Bornscheuer 1982 and Vandepitte et al. 1980. The ASME and API codes allow the use of larger capacity reduction factors for shells with smaller length parameter M and smaller radius-to-thickness ratio R/t; i.e., a smaller reduction of the elastic buckling stress is permissible for shorter and thicker shells. Figure 8 also shows that the values recommended by all the design codes are conservative, since they are closer to the lower than the upper bound of the test data. Moreover, the ASME-N284 recommendations appear to be the most conservative of all. For this reason, the SCANS computer program use the ASME recommendations.

When the actual elastic buckling stress, i.e.,the theoretical elastic buckling stress multiplied by the capacity reduction factor, has a magnitude greater than the linear elastic strength or the proportional limit of the shell material, the effect of plasticity should be included, using a value less than 1.0 for the plasticity reduction factor in Eq. (1). Analyses have shown that the plasticity reduction factor depends on both the elastic and plastic properties of the shell material, decreasing with decreasing values of the ratio between the elastic and plastic moduli of the shell materials. Several simple formulas have been proposed for the determination of this factor for work-hardening materials with a smooth stress-strain curve in the plastic range. Three of these formulas have been compared in Lo et al. 1989. Since the ASME-N284 code does not provide the plasticity reduction factor for stainless steels, the SCANS computer program uses the most conservative of these three formulas to calculate the factor; i.e.,

$$\eta = E_t/E, \qquad (3)$$

where E_t is the tangent modulus of the stress-strain curve at the actual plastic buckling stress, and E is the elastic or Young's modulus. In addition, SCANS assumes that the stress-strain relation has the following general form in the plastic range:

$$\sigma = \sigma_0 \varepsilon^m, \qquad (4)$$

where σ and ε are true stress and strain, respectively; and σ_0 and m are coefficients to be determined by curve fitting.

For the plasticity reduction factors of carbon steels, SCANS uses the formulas provided by ASME-N284. The formulas were obtained from test results. The same approach was used in the German

and European codes, as discussed in Bornscheuer 1982 and Vandepitte et al. 1980. Figure 9 compares the plasticity factors assumed by the various design codes. The results are presented in the form of normalized limiting stress versus the inverse of normalized actual elastic buckling stress, λ. The stress used for the normalization is the material's yield stress, σ_y. The limiting stress is the actual buckling stress of the shell, either elastic or plastic. The normalized elastic buckling stress parameter, λ, is defined as follows:

$$\lambda = [\sigma_y/(\alpha\, \sigma_e)]^{1/2} \tag{5}$$

A value of λ less than, equal to, or greater than 1.0 indicates that the material's yield stress is respectively greater than, equal to, or less than the actual elastic buckling stress. The shell tends to buckle elastically when the λ value is much greater than 1.0, because the actual elastic buckling stress is much lower than the yield stress. Thus in Fig. 9, the limiting stress curve in this range of large λ values is the elastic buckling stress curve. On the other hand, in the range of λ values close to or less than 1.0, where the actual elastic buckling stress exceeds the elastic or proportional limit, the shell would buckle plastically, and the actual plastic buckling stress determines the limiting stress curve in Fig. 9. For λ values near zero, both the actual elastic and plastic buckling stresses would exceed the yield stress of the material. Then the plastic deformation of the material rather than the buckling of the shell might set the limit on the permissible stress in the shell. For this reason some design codes do not allow the buckling stress limit to exceed the yield stress.

The analytical expression for the limit stress curves in the various λ ranges of Fig. 9 can be obtained from Eqs. (1) and (5), i.e.,

for elastic buckling,

$$\sigma_\ell/\sigma_y = \alpha\, \sigma_e/\sigma_y = 1/\lambda^2; \tag{6}$$

for plastic buckling,

$$\sigma_\ell/\sigma_y = \eta\, \alpha\, \sigma_e/\sigma_y = \eta/\lambda^2 \tag{7}$$

Equation (6) shows that only a single curve in Fig. 9 is needed to define the actual elastic buckling stress for all the design codes, because Eq. (6) is independent of α,which is shown in Fig. 8 to have greatly different values among the various design codes. Similarly, Eq. (7) shows only the effect of η and not α. Thus, the actual plastic buckling stress curves in Fig. 9 provide a true comparison of the η values used in the various design codes. In the same figure, available buckling test data are also shown. Similar to the observation just made on the α values, the η values used by the various design codes are also conservative, i.e., lying closer to the lower than the upper bound of the test data range. The test data, presented in Bornscheuer 1982 and Vandepitte et al. 1980 were obtained for several materials: steel, aluminum, and brass. These test data indicated that the plastic buckling stress after being normalized using the yield stress of the shell material is actually not very material dependent. Figure 9 also presents two analytical plastic buckling stresses obtained for stainless steel shells using the BOSOR5 computer program, which was developed specifically for buckling analysis Bushnell 1986. The BOSOR5 results agree with the others presented in the same figure.

The information of Figs. 8 and 9 is combined in Fig. 10 to show the relation between the actual axial buckling stress and the R/t ratio of the circular cylindrical shell. The results indicate that when the R/t ratio is greater than 450, the shell fails definitely by elastic buckling; when the R/t ratio is between 20 and 450, the shell tends to fail by plastic buckling; and for R/t less than 20, the shell material might yield before the shell structure would buckle. This information is useful as a rule of thumb to determine the need for buckling analysis. The results in Fig. 10 again demonstrate that, among all the design codes studied herein, the ASME-N284 code used in the SCANS computer program provides the most conservative estimate of the buckling stress.

APPLICATION OF SCANS FOR LEAD SLUMP AND BUCKLING ANALYSIS

The SCANS capabilities described in the foregoing sections for lead slump and buckling analyses have been applied to the buckling analysis of the sample rail cask and limiter depicted in Figs. 4 and 5. Table 2 gives the results of this study for the inner steel shell of the cask undergoing a 30-ft end-on drop. Results are shown with and without the lead slump effect. The outer shell is not analyzed, because, compared to the inner shell, it has a smaller R/t ratio (14.7 vs 20.5) and because a tensile rather than a compressive hoop stress is caused by the lead slump. According to the understanding of buckling presented in this paper, the yielding of the material rather than the buckling of the structure would govern the design of the outer shell.

The results in Table 2 show that the inner shell has a much greater tendency to buckle with lead slump than without it. Moreover, the results reveal that the inner shell would not provide sufficient margin of safety for buckling if lead slump occurs. The ASME code requires a safety factor of 1.34 for buckling under accident conditions. Thus, these sample results have demonstrated the significance of considering lead slump in buckling analyses of casks.

SUMMARY AND CONCLUSIONS

This paper has discussed the effect and significance of lead slump and buckling in the structural design of casks for shipment and storage of radioactive materials. The paper also describes briefly the bases and methods used in the IBM-PC computer program SCANS for these analyses. To demonstrate the verifications of these analysis capabilities, SCANS results have been compared to those of tests and other computer programs. Finally, by applying the SCANS program to the analysis of a 30-ft end-on impact of a sample rail cask, this paper has demonstrated the importance of considering lead slump in buckling analyses.

REFERENCES

Bornscheuer, R.W., *To the Problem of Buckling Safety of Shells in the Plastic Range, Buckling of Shells*, E. Ramm, Ed., Springer-Verlag, (1982).

Brush, D.O., and Almroth, B.O., *Buckling of Bars, Plates and Shells*, McGraw-Hill, (1975).

Bushnell, D., *BOSOR5—Program for Buckling of Complex, Branched Shells of Revolution Including Large Deflections, Plasticity, and Creep, Structural Analysis Systems*, Vol. 2, A. Niku-Lari, Ed., Pergamon Press, (1986).

Chun, R.C., Lo, T.Y., Mok, G.C., and Witte, M.C., *SCANS Theory Manual, Vol.3, Lead Slump in Impact Analysis and Verification of Impact Analysis*, NUREG/CR-4544, Vol. 3, (1989).

Lo, T.Y., et al., *SCANS Theory Manual, Vol. 6, Buckling of Circular Cylindrical Shells*, NUREG/CR-4554, to be published in 1989.

Mok, G.C., Chun, R.C., Lo, T.Y., and Witte, M.C., *The Analysis of Lead Slump Effects in Shipping Casks for Radioactive Materials*, paper to be presented at the ASME-JSME Joint Conference on Nuclear Pipings and Pressure Vessels, Honolulu, HI, (1989).

Vandepitte, D., and Rathe, J., *Buckling of Circular Cylindrical Shells Under Axial Load in Elastic-Plastic Region*, Stahlbau, Vol. 49, (1980).

Table 1. Comparison of results for casks with bonded and unbonded lead shield as obtained using the NIKE and SCANS computer programs (Sample Problem, 90-degree impact).

Shield Type	Elastic Properties of Lead Shield: Young's Modulus (psi)	Elastic Properties of Lead Shield: Poisson's Ratio	Analysis Method	Stresses (psi) at Axial Location 22" from Impact End: Inner Steel Shell: Axial Stress	Inner Steel Shell: Radial Stress	Inner Steel Shell: Circ Stress	Lead Shield: Axial Stress	Lead Shield: Radial Stress	Lead Shield: Circ Stress	Outer Steel Shell: Axial Stress	Outer Steel Shell: Radial Stress	Outer Steel Shell: Circ Stress
Bonded	25000	0.43	SCANS	-6644	0	0	-6	0	0	-6644	0	0
			NIKE	-7550	-18	-440	-18	-12	-11	-5050	-17	175
Unbonded	25000	0.43	SCANS	-13199	0	-32658	-2788	-1660	-1901	-1200	0	19450
			NIKE	-7500	-600	-26000	-3330	-1190	-1520	-1300	-300	18000
Bonded	2220000	0.43	SCANS	-6438	0	0	-505	0	0	-6438	0	0
			NIKE	-6193	5	1166	-467	-22	-15	-4715	-36	875
Unbonded	2220000	0.43	SCANS	-4115	0	-412	-3296	-581	-1530	-3487	0	1824
			NIKE	-4771	-24	-601	-3184	-103	-1262	-2355	-85	2356

Note: The lead property values used to obtain the results in this table are for parametric study only. The current SCANS program uses a different set of values for the properties and, therefore, will not reproduce the SCANS results shown herein.

Table 2. Results of SCANS buckling analysis of inner stainless steel shell of sample rail cask (30-ft, 90-degree impact)

Stress Comp	Max Stress (psi)	Theoretical Elastic Buck Stress (psi)	Cap. Reduct. Factor	Plast. Reduct. Factor	Actual Buckling Stress (psi)	Factor of Safety	Maximum Interaction Stress Ratio (> 1 : buckle)
Case 1: Bonded Lead Shield (without lead slump)							
Axial	5045	826420	0.321	0.118	31234	1.0	0.019
Hoop	0	49896	0.8	0.544	21730	1.34	0.026
Shear	0	16415	0.8	0.103	16415		
Case 2: Unbonded Lead Shield (with lead slump)							
Axial	12585	826420	0.321	0.118	31234	1.0	0.832
Hoop	30041	49896	0.8	0.544	21730	1.34	1.494 (Buckle)
Shear	0	16415	0.8	0.103	16415		

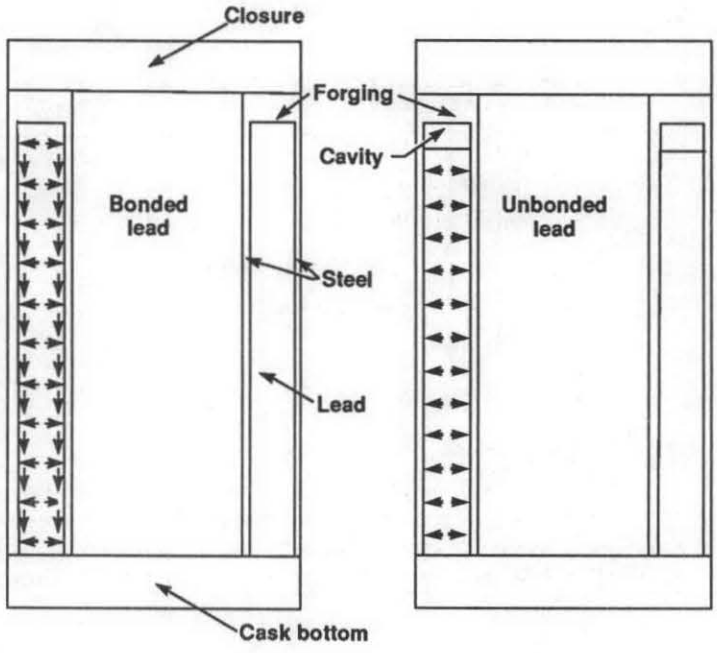

Figure 1. Cause and effect of lead slump.

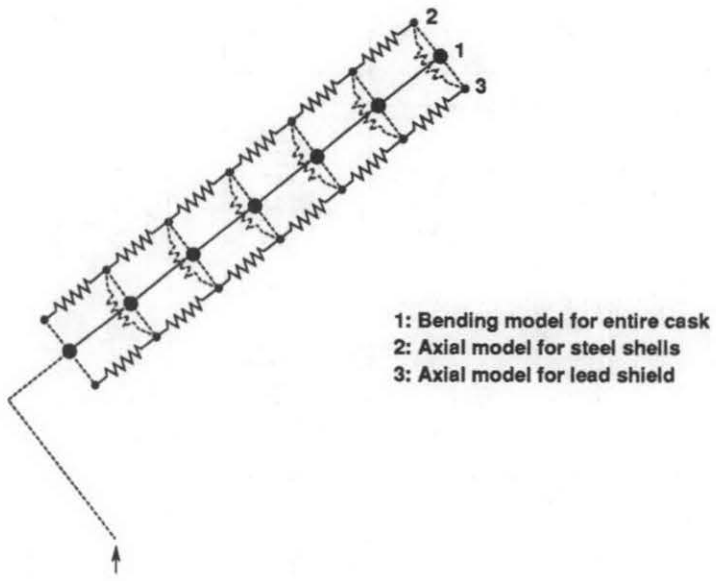

Figure 2. SCANS model for cask with unbonded lead shield.

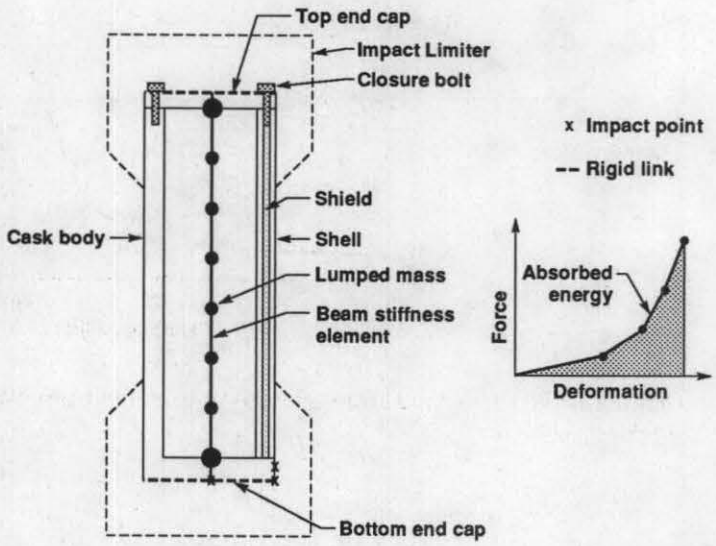

Figure 3. SCANS model for cask with bonded lead shield.

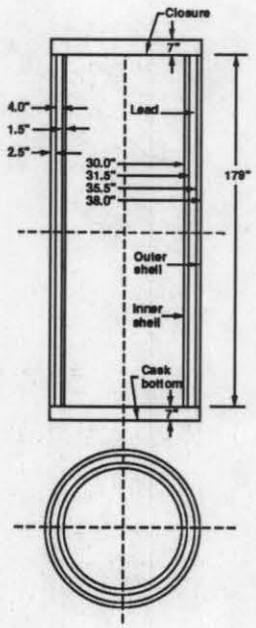

Figure 4. Sample rail cask for lead slump analysis.

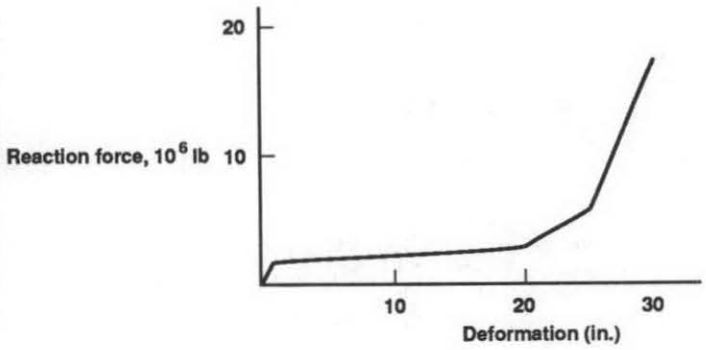

Figure 5. Force-deformation relation of impact limiters of sample rail cask.

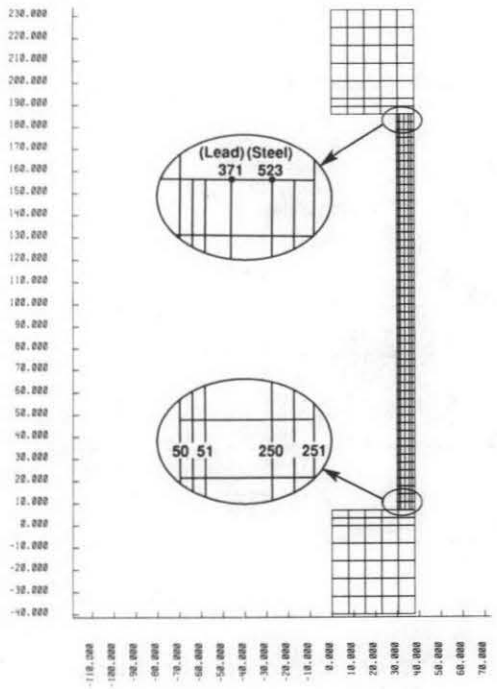

Figure 6. NIKE model of sample rail cask with impact limiters.

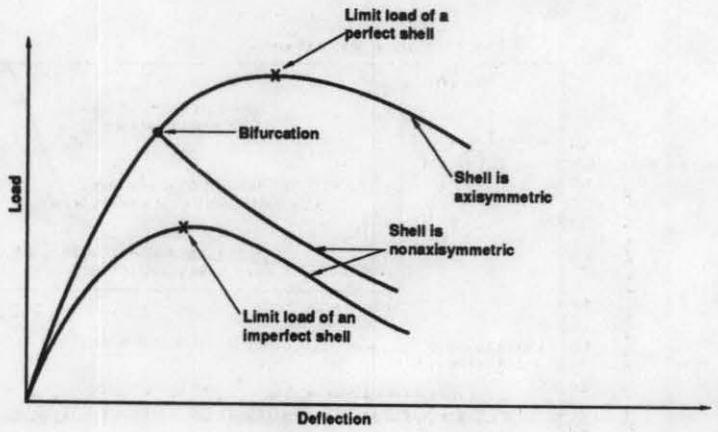

Figure 7. Buckling of a circular cylindrical shell.

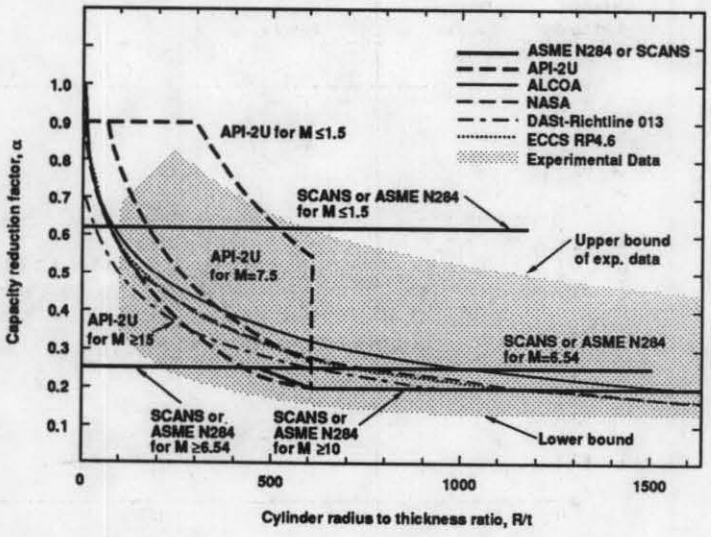

Figure 8. Dependence of capacity reduction factor on R/t ratio as specified by various design formulas for elastic buckling of circular shell under axial compression.

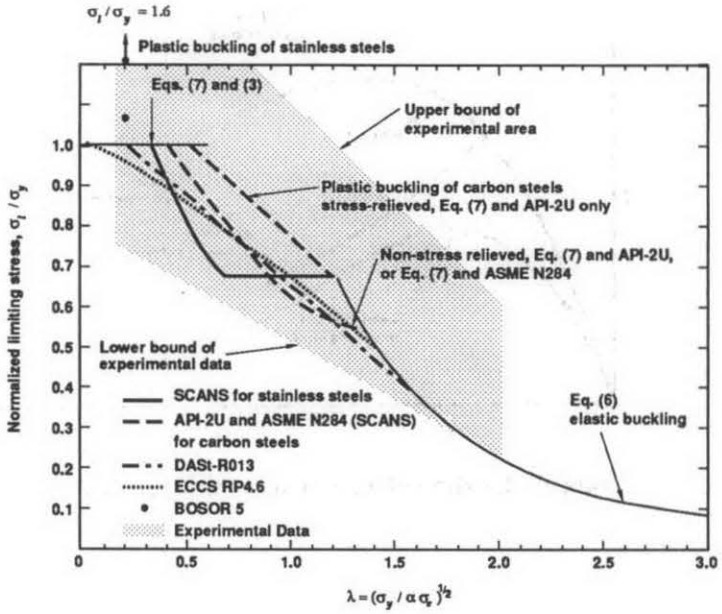

Figure 9. Dependence of limiting stress on failure mode and actual elastic buckling stress as specified by various design formulas for circular shell under axial compression.

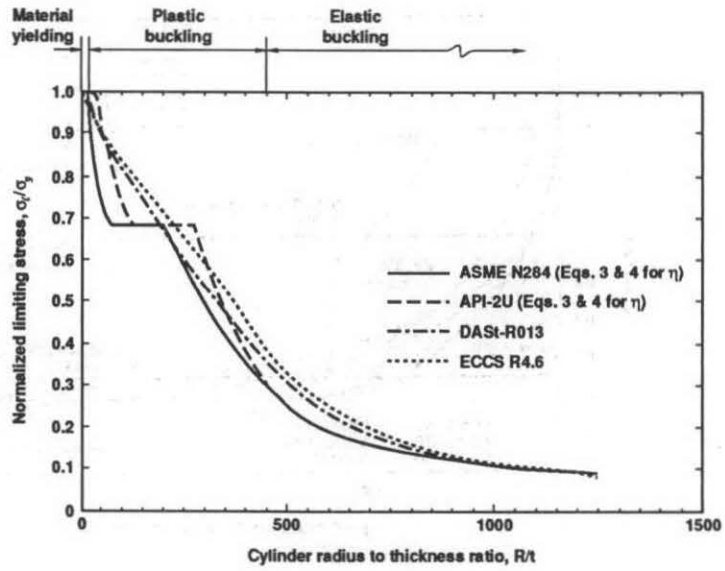

Figure 10. Dependence axial limiting stress and failure mode on radius-to-thickness ratio of circular cylindrical shell.